Structure/Control Design Synthesis of Active Flutter Suppression System by Goal Programming

Shinji Suzuki and Seiji Matsuda
University of Tokyo, Bunkyo-ku, Tokyo 113, Japan

The simultaneous design of the structure and control for a typical wing section with a trailing control surface is considered. Since the original structure usually has inadequate dynamic characteristics for active control, design parameters must be optimally modified. Full-state feedback control gains are designed using the linear quadratic Gaussian regulator theory at the design airspeed; this is the only control design parameter. A typical wing section with a trailing control surface is examined as a design example, and then both structure and control design parameters are optimized in accordance with the following prioritized design requirements: 1) the flutter speed of an initial open-loop system is maintained, 2) the stability characteristics of a closed-loop system are obtained over a wide range of flight speed, 3) the control surface deflection angle is restrained, and 4) the degree of structural design changes is minimized. The sequential goal programming method is successfully applied to optimize these multidisciplinary design requirements.

Introduction

ACTIVE flutter suppression has been recognized as a means to improve wing damping characteristics without increasing structural stiffness and without adding mass balancing. Several techniques of control synthesis of flutter suppression have been presented.[1-4] In these studies, analytical and experimental results reveal that there is an inter-relationship between structural design and control synthesis.[5-7] Generally, since the installation of an active control system is not taken into account in structural design, the structural dynamic characteristics are sometimes altered in the process of control design. Consequently, it has been suggested that structure/control design must be integrated at an early vehicle design stage.[5,6]

Numerical optimization of simultaneous structure/control design has been applied to structures in space[8-10]; however, this approach has not been used in the design of an active flutter suppression system due to several complex difficulties, e.g., control systems must operate in various flight conditions resulting from the system characteristics varying with the dynamic pressure and sufficient open-loop characteristics must be provided against a control system failure. Numerical optimization procedures handle these problems by treating them as design constraints. Since constraints conflict with one another, it is difficult to use this technique to obtain feasible solutions satisfying all constraints. Reference 10 manages to solve the dilemma using a method that initially relaxes the original constraints to provide an initial solution and then recovers them iteratively.

In this research, goal programming (GP) is applied to optimize the structure/control design parameters for an active flutter suppression system. Goal programming, developed for use in mathematical economics, deals with design constraints as achievement goals, using priority assignments to solve conflicting multiple goals.[11-13] The simplex algorithm can be efficiently applied to GP for linearized problems; therefore, a nonlinear GP problem can be sequentially approximated as a linearized GP problem to obtain the optimal solution using the simplex algorithm. This approach is named the sequential GP method. Whereas the sequential linear programming method using a sequentially applied simplex algorithm has been reported to be an efficient and reliable method for nonlinear optimization problems,[10] the presented sequential GP method has never been applied in structure/control design synthesis.

A typical wing section is considered as a design example. This section was presented as the worst-case design example in Ref. 14. Because of lack of controllability in the original structural design, the optimal regulator failed to produce adequate

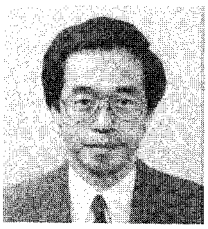

Shinji Suzuki is an Associate Professor of Aeronautical Engineering at the University of Tokyo. He received his doctorate from the University of Tokyo in 1986. From 1979 to 1986, he worked for Toyota Central R&D Laboratories on noise and vibration analysis of vehicle structures. His current interest is analysis and synthesis of flexible spacecraft and aircraft with control systems. He is a Member of AIAA.

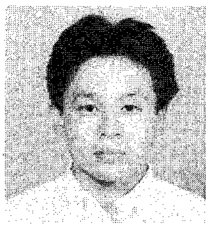

Seiji Matsuda received his B.S. and M.S. in aeronautical engineering from the University of Tokyo in 1988 and 1990, respectively. His research in the university was the simultaneous structure and control design for active flutter suppression systems. He currently works for Nissan Motor Company, Ltd., as an engineer in the Space System Department, Aerospace Division.

Received June 25, 1990; presented as Paper 90-3325 at the AIAA Guidance, Navigation, and Control Conference, Portland, OR, Aug. 20–22, 1990; revision received Oct. 12, 1990.

control. Reference 14 solved this problem by adding a leading-edge control surface, whereas this paper uses GP to determine optimal modification of both structure and control design parameters. The elastic axis location, the hinge line location, the distance from elastic axis to mass center, and the distance from hinge line to control surface mass center are selected as structural parameters. The full-state feedback control gains are obtained using linear quadratic Gaussian regulator (LQGR) theory; thus, the only control parameter is the design speed where the control gains are determined. It should be noted that the feedback gains are optimally calculated in each design modification.

An optimal modification was successfully obtained in accordance with the following design concepts: 1) the flutter speed of the initial open-loop design is maintained, 2) the stability characteristics of a closed-loop system are obtained over a wide range of flight speed, 3) the deflection angle of the control surface is restrained, and 4) the degree of structural design changes is minimized. Although Ref. 5 dealt with similar research, it did not explicitly utilize these complex design requirements.

Typical Section Model

Figure 1 shows a typical two-dimensional wing section elastically supported in an airstream U. It has three degrees of freedom, plunge h, pitch α, and trailing-edge control surface deflection β. Linear and torsion springs at the elastic axis act to restrain motion in plunge and pitch, and the torsion spring acts at the control surface hinge line. The flutter equation can be written in the following form:

$$M_s \ddot{x}_s = -K_s x_s + F_a + F_g + B_s u \qquad x_s^T = [h/b \quad \alpha \quad \beta] \tag{1}$$

where M_s and K_s are structural mass and stiffness matrices, and F_a and F_g are vectors of aerodynamic and gust loads. Control torque $B_s u$ around the hinge line is generated by control input u. The flow is assumed incompressible, and the unsteady characteristics in aerodynamic loads F_a and F_g are expressed using the Padé model.[15,16]

The random gust with a vertical velocity w_g is adopted as a disturbance of the system. The gust model is expressed as

$$\dot{w}_g = -(1/T_g) w_g + w \tag{2}$$

where T_g and w are time constants of the gust model and white noise input, respectively. When the variance of the vertical velocity w_g is written as σ^2, the intensity of the white noise is defined as $2\sigma^2 T_g$.

Arranging Eqs. (1) and (2) gives the state-space equations of the flutter system:

$$\dot{x}_p = A x_p + B u + w_p \qquad x_p^T = [x_s \quad \dot{x}_s \quad x_a \quad x_g \quad w_g] \tag{3}$$

where x_a and x_g are augmented state variables expressing the unsteady aerodynamic loads and gust, and w_p is a white noise vector of intensity matrix V.

Details of the M_s, K_s, F_a, F_g, B_s, A, and B matrices can be found in Refs. 14-16.

Control Law Synthesis Method

Linear quadratic Gaussian regulator theory is applied to determine full-state feedback control gains. Using steady-state LQGR, the cost function has the form:

$$J = \lim_{t\to\infty} E\left[x_p^T(t) R_1 x_p(t) + u^T(t) R_2 u(t)\right] \tag{4}$$

where $E[\;]$ denotes the expected value operator, and R_1 and R_2 are weighting matrices.

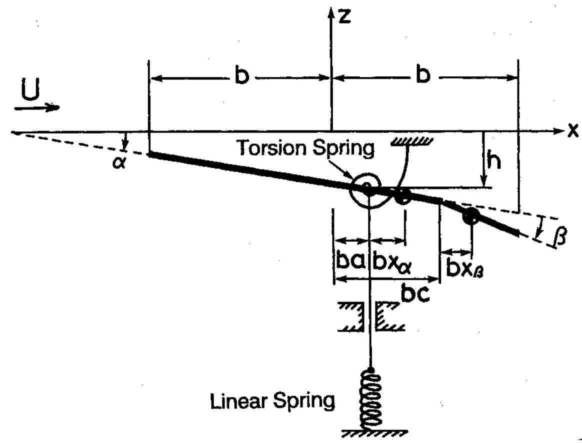

Fig. 1 Typical wing section with control surface.

The optimal full-state feedback control law is given as[17]

$$u = -F x_p \tag{5}$$

$$F = R_2^{-1} B^T P \tag{6}$$

where F is the feedback control gain vector, and P is the positive definite symmetric matrix of the solution to the following steady-state Riccati matrix equation:

$$R_1 - PBR_2^{-1}B^T P + PA + A^T P = 0 \tag{7}$$

Dynamic characteristics of the system in a stochastic process are evaluated using covariances of state variables x_p. The covariance matrix in steady state is defined as[17]

$$Q = \lim_{t\to\infty} E[x_p x_p^T] \tag{8}$$

The covariance matrix Q is solved by the Lyapunov matrix equation:

$$(A - BF)Q + Q(A - BF)^T + V = 0 \tag{9}$$

where V is the intensity matrix of the white noise w_p in Eq. (3).

Initial Design Characteristics

Table 1 lists the structural and geometric parameters used and represents the worst-case design example.[14] Figure 2a shows the eigenvalues of the open-loop system (root locus) as a function of nondimensional airspeed U^* ($=U/b\omega_\alpha$, ω_α is the natural frequency of the pitch mode). The x and y axes are the nondimensional airspeed and the nondimensional eigenvalues λ^* ($=\lambda/\omega_\alpha$). When the real part of an eigenvalue becomes positive, the system becomes unstable. Therefore, the plunge h mode becomes unstable above the flutter speed, $U_f^* = 2.98$. The shaded regions in Fig. 2 indicate where the system is unstable.

Table 1 Typical wing section parameters

ω_α	Natural frequency associated with α	100 rad/s
ω_β	Natural frequency associated with β	300 rad/s
ω_h	Natural frequency associated with h	50 rad/s
μ	Section mass ratio	40
a	[a]Elastic axis location /b	−0.4
c	[a]Hinge line location /b	0.5
χ_α	[a]Distance from elastic axis to mass center /b	0.2
γ_α^2	Radius of gyration associated with α	0.25
χ_β	[a]Distance from hinge line to control surface mass center /b	0.0125
γ_β^2	Radius of gyration associated with β	0.00625
σ^2	Variance of gust velocity	1.0
T_g	Time constant of gust model	$3/20\pi$

[a]Denotes structural design parameters.

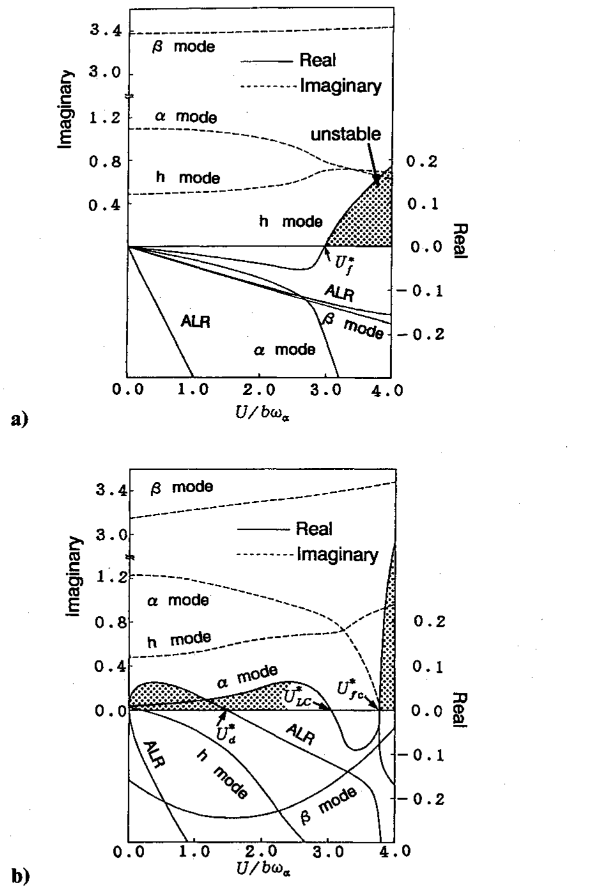

Fig. 2 Locus of eigenvalues of initial design (nondimensionalized by ω_α) as a function of $U/b\omega_\alpha$: a) open-loop system; b) closed-loop system.

A control law was designed at the condition of $U^* = 3.25$, i.e., the design airspeed U_D^*, a speed at which the open-loop system was unstable. Although there are two weighting matrices in Eq. (4), only the weighting matrix R_2 is necessary to assure stability of the closed-loop system. Therefore, R_1 and R_2 were chosen to be a zero and a unity matrix, respectively. Figure 2b shows the eigenvalues of the closed-loop system when the feedback gains were held constant at the nondesign airspeeds. The closed-loop system was stable around the design airspeed U_D^*, and the closed-loop flutter speed U_{fc}^* increased to 3.80. However, in the closed-loop system, two unstable regions occur below the closed-loop flutter speed U_{fc}^*, as shown in Fig. 2b. One is due to instability of the pitch α mode below U_{LC}^*, and the other is due to the divergence of one of the aerodynamic lag roots (ALRs) below U_d^*. Note that ALRs were introduced to model the unsteady characteristics in aerodynamic loads.

Figure 3 shows the eigenvalues of the open-loop and closed-loop systems in a different style. The x and y axes are the real and imaginary parts of the dimensionless eigenvalues. A system becomes unstable when the eigenvalue is located to the right side of 0.0 on the real axis.

Reference 14 found that the pitch mode instability in the closed-loop system was attributable to the poor controllability of the wing section by the trailing-edge control at around U_{LC}^*. Uncontrollability of the mode was indicated by pole-zero proximity of the loop transfer matrix. These poles (eigenvalues) and zeros are calculated from the denominators and numerators of the loop transfer matrix, respectively. In this case, the pitch mode zeros approximate the plunge mode poles when $U^* \simeq 3.0$. This proximity is associated with stabilization difficulties in the closed-loop system. Reference 14 added a leading-edge control surface to improve uncontrollability, causing the pitch mode zeros and the plunge mode poles to

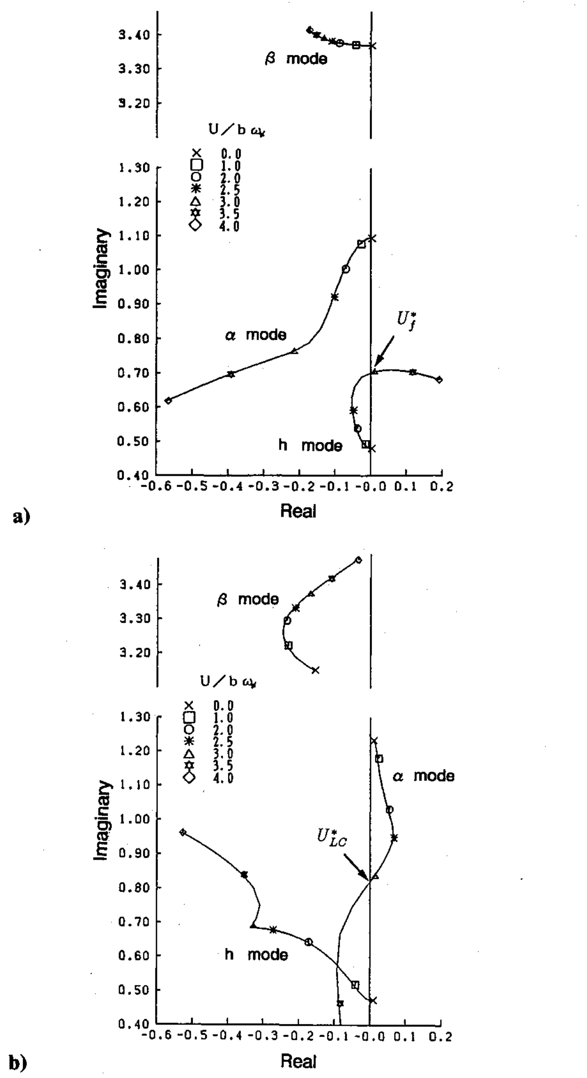

Fig. 3 Locus of nondimensional eigenvalues of initial design: a) open-loop system; b) closed-loop system.

separate. Contrary to this solution, design modifications of the wing section are proposed here. The proposed approach is considered superior because the system has adequate dynamic characteristics for active control without adding complex control devices.

Sensitivity Analysis

The derivatives of eigenvalues and covariances with respect to design parameters are effective values with which to gain insight into structure and control design modifications. These derivatives may be calculated by finite differences, although the numerical computations are quite expensive and time consuming. Computational efficiency is required in the design optimization described in the next section because the derivatives associated with design parameters must be calculated in each design cycle; thus, analytical derivatives are applied with the application method called sensitivity analysis.[18]

The derivative with respect to a design parameter p, for ith eigenvalue of the system matrix A, has the form[19]

$$\frac{\partial \lambda_i}{\partial p} = y_i^T \frac{\partial A}{\partial p} x_i \tag{10}$$

where x_i and y_i are the ith right and left eigenvectors of the system matrix A, respectively, and these vectors are normalized as $y_i^T x_i = 1$. This gives the derivatives of the open-loop eigenvalues, whereas the substitution of $A - BF$ into A

in Eq. (10) yields those of the closed-loop system:

$$\frac{\partial \lambda_i^c}{\partial p} = y_i^T \left(\frac{\partial A}{\partial p} - \frac{\partial B}{\partial p} F - B \frac{\partial F}{\partial p} \right) x_i \tag{11}$$

where $\partial F / \partial p$ is the derivative matrix of the optimal feedback control gains. Since the optimal feedback gains are altered due to the design parameter change, the derivative $\partial F / \partial p$ must be evaluated. Using Eq. (6), under the assumption that R_1 and R_2 are independent of p, results in

$$\frac{\partial F}{\partial p} = R_2^{-1} \frac{\partial B^T}{\partial p} P + R_2^{-1} B^T \frac{\partial P}{\partial p} \tag{12}$$

Differentiating Eq. (7) allows the derivatives of the Riccati solution to be obtained from

$$\frac{\partial P}{\partial p} A_c + A_c \frac{\partial P}{\partial p} + D_1 = 0$$

$$A_c = A - BF \tag{13}$$

$$D_1 = -P \frac{\partial B}{\partial p} F - F^T \frac{\partial B^T}{\partial p} P + \frac{\partial A^T}{\partial p} P + P \frac{\partial A}{\partial p}$$

where Eq. (13) is in the form of the Lyapunov equation.[9]

The derivative of the covariance matrix is calculated from the Lyapunov equation:

$$A_c \frac{\partial Q}{\partial p} + \frac{\partial Q}{\partial p} A_c + D_2 = 0$$

$$D_2 = \frac{\partial A_c}{\partial p} Q + Q \frac{\partial A_c^T}{\partial p} \tag{14}$$

obtained from Eq. (9), assuming that V is independent of p.

Using this sensitivity analysis, the derivatives of the eigenvalues with respect to several design parameters in Table 1 were calculated. Figure 4 shows the change of root loci of the open- and closed-loop systems when the value of the center of gravity χ_α was varied $\pm 10\%$ from the initial value. Notice that the shift of the center of gravity in the closed-loop system to the aft of the section extends the stable boundary, yet slightly decreases the flutter speed of the open-loop system. This result indicates that it is difficult to improve the closed-loop system characteristics without decreasing the flutter speed of the open-loop system. The flutter speed of the open-loop system should be maintained to protect against a failure of the control system.

Design Optimization by Goal Programming

As shown in the previous section, it is difficult to find a sufficient design that satisfies both open- and closed-loop characteristics, and, subsequently, a numerical optimization approach is needed to obtain the optimal modifications. In this study, χ_α, χ_β, c, and a were chosen as structural design parameters (see Table 1), being nondimensionalized by a half chord length b. In addition, the design speed was selected as a control design parameter, since at that speed the LQGR produced optimal feedback control gains.

The numerical optimization was carried out in accordance with the following prioritized design requirements.

Open-Loop Characteristics

To obtain sufficient open-loop characteristics against a failure of the control system, the flutter speed of the initial design must be maintained. This requirement is represented as follows:

$$\mathrm{Re}[\lambda_i^*] < 0.0, \qquad i = 1,\ldots,11 \quad \text{at} \quad U^* = 1.0, 3.0 \tag{15}$$

where λ_i^* is the dimensionless ith open-loop eigenvalue of the system matrix A, and Re[ ] denotes the real part of a complex value. The sensitivity analysis showed that the stability characteristics in the open-loop system did not drastically change; consequently, the constraints were only specified at two discrete speed points, whereas the eigenvalues vary continuously with the flight speed.

Closed-Loop Characteristics

To obtain the stability characteristics of the closed-loop system over a wide range of flight speed, these requirements are written as

$$\mathrm{Re}[\lambda_i^{c*}] < 0.0, \quad i = 1,\ldots,11 \quad \text{at} \quad U^* = 1.0, 2.6, 3.0, 3.8 \tag{16}$$

$$\mathrm{Re}[\lambda_i^{c*}] < -0.1, \quad i = 1,\ldots,11 \quad \text{at} \quad U^* = 2.1, 2.2, 2.3, 2.4, 2.5 \tag{17}$$

where λ_i^{c*} is the ith closed-loop eigenvalue of the system matrix A_c. Equation (17) has strict constraints to assure robust control system characteristics since the initial design had poor controllability at that airspeed range ($2.1 \sim 2.5$).

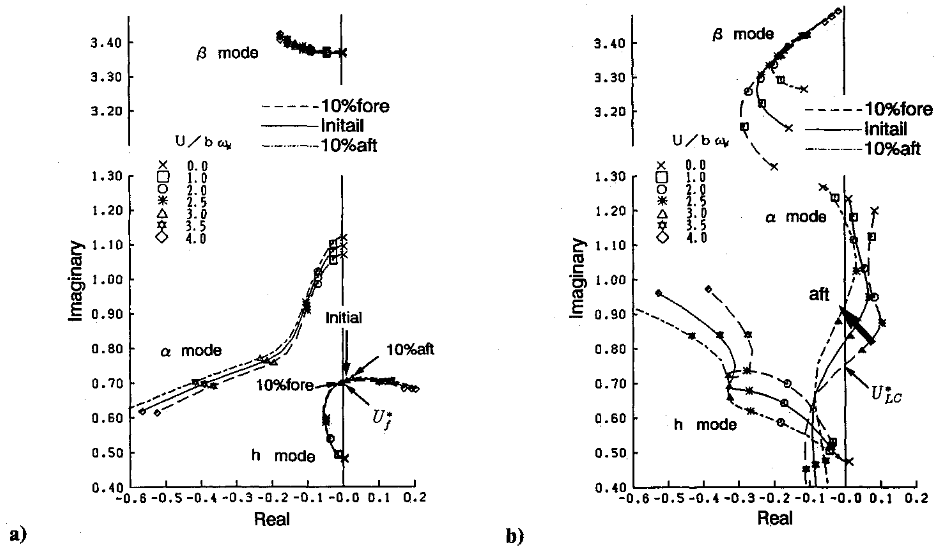

Fig. 4 Change of root loci by movement of mass center: a) open-loop system; b) closed-loop system.

Restraint of the Control Surface Deflection Angle

The deflection angle of the control surface should be physically restrained. These restraints are given by

$$\mathrm{Var}[\beta] < 0.001 \quad \text{at} \quad U^* = 1.0, 2.0, 2.1, 2.2, 2.3, 2.4, 2.5, 2.6, 3.0, 3.8 \tag{18}$$

where $\mathrm{Var}[\beta]$ is the steady-state covariance of the deflection angle presented in Eq. (9).

Restraint of Structural Design Changes

The degree of structural design changes should be minimum; thus, each design parameter value should be set close to its initial value.

Goal programming[11-13] is introduced as a method to numerically optimize these design requirements. Although this approach is not commonly used by dynamic and control engineers, GP should be considered since it has several advantages. First, GP deals with constraints as goals to be achieved; therefore, it is not necessary to obtain an initial feasible design that satisfies all the constraints. Second, the simplex algorithm can be used to efficiently solve linear GP problems. For GP nonlinear problems that have a large number of goals, the sequentially applied simplex algorithm to linearized GP problems yields an efficient and reliable solving method.

A general nonlinear optimization problem can be expressed as

$$\text{minimize} \qquad f(x) \tag{19}$$

$$\text{subject to} \qquad g_j(x)\{\leq, =, \geq\}0.0, \qquad j = 1, \ldots, m \tag{20}$$

where x is the design parameter vector. In the presented study, the objective function f represents a minimum design change requirement and the constraint functions g_j represent both the stability requirement for the open- and closed-loop systems and the restriction of the control surface deflection angle.

Sensitivity analysis makes it possible to decompose a nonlinear problem into a linear optimization problem:

$$\text{minimize} \qquad Cx \tag{21}$$

$$\text{subject to} \qquad Z_j x\{\leq, =, \geq\} b_j, \qquad j = 1, \ldots, m \tag{22}$$

$$x_L \leq x \leq x_U \tag{23}$$

where C and Z_j are $1 \times n$ coefficient matrices, and Eq. (23) defines the range that each design parameter can be moved and still assure the linearity assumption. The variables x_L and x_U denote lower and upper limit vectors, respectively.

In the GP approach, the left polynomial of the ith restriction in Eq. (22) becomes an objective function having goal b_j, and if the original objective function Eq. (21) is the design change degree (given as the difference from the initial design parameters), then the degree of difference is reduced and each design parameter becomes closer to the initial values, i.e., the goals. As a result, Eqs. (21-23) are transformed into the following equivalent forms:

$$\text{minimize} \qquad \sum_{l=1}^{L} P_l \left[\sum_{j \in I_l} (w_j^+ d_j^+ + w_j^- d_j^-) \right] \tag{24}$$

$$\text{subject to} \qquad Z_j x - d_j^+ + d_j^- = b_j \qquad j = 1, \ldots, m' \tag{25}$$

$$\text{all} \qquad d_j^+, d_j^- \geq 0 \tag{26}$$

$$x_L \leq x \leq x_U \tag{27}$$

where d_j^+ and d_j^- denote the overachievement and the underachievement of the jth goal. In Eq. (24), P_l represents the priority of the goals, and w_j^+ and w_j^- are weights in the same priority level I_l. The goals are scaled by the importance of their priority level. An appropriate choice of w_j^+ and w_j^- makes it possible to deal with various types of constraints (see Ref. 13). For example, if the objective values are set to be less than the goals, as in Eqs. (15-18), w_j^+ and w_j^- are chosen to be a positive integer and 0, respectively. The GP formulated problem can now be solved using the conventional simplex algorithm.

Table 2 Cost function

Priority number l	Value P_l	Weights (w_i^+, w_i^-)	Requirement
1	10^6	(5,0)	$\mathrm{Re}[\lambda_i^*] < 0.0$
		(1,0)	$\mathrm{Re}[\lambda_i^{c*}] < 0.0$
		(1,0)	$\mathrm{Re}[\lambda_i^{c*}] < -1.0$
2	10^3	(1,0)	$\mathrm{Var}[\beta] < 0.001$
3	1	(1,1)	Minimum design modification

The priority levels previously discussed in this section are listed in Table 2, with the values of P_l, w_j^+, and w_j^- also presented. The design procedure is illustrated by the flowchart in Fig. 5. In each design cycle, the sensitivity analysis is used to achieve a linear problem, and then each design parameter is optimally modified by GP within the design parameter's range. Goal programming incorporates the optimal feedback control gains that are calculated by LQGR theory in each design cycle.

Numerical Results

The optimization procedure was used to modify the typical wing section design parameters. Figure 6 shows the design cycle histories of the objective functions in goal programming.

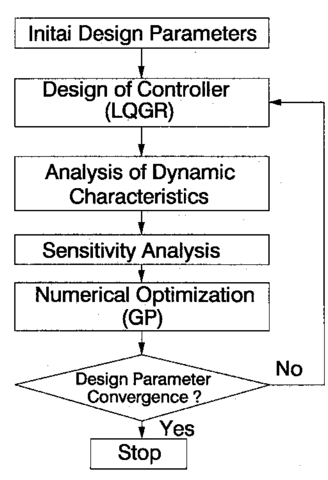

Fig. 5 Design cycle flow chart.

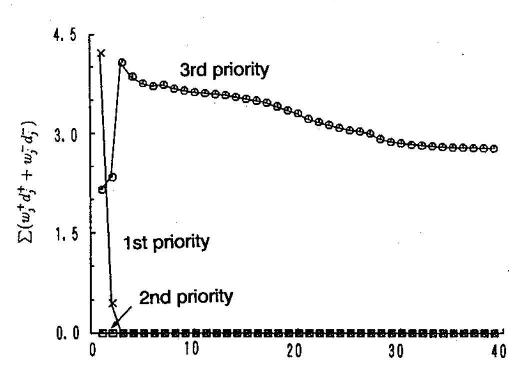

Fig. 6 Design cycle deviation histories for priority level.

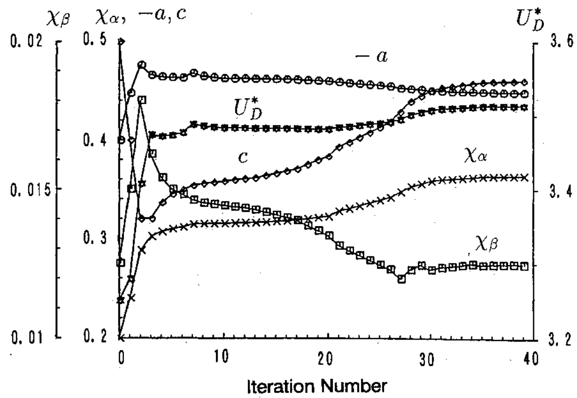

Fig. 7 Design parameter histories.

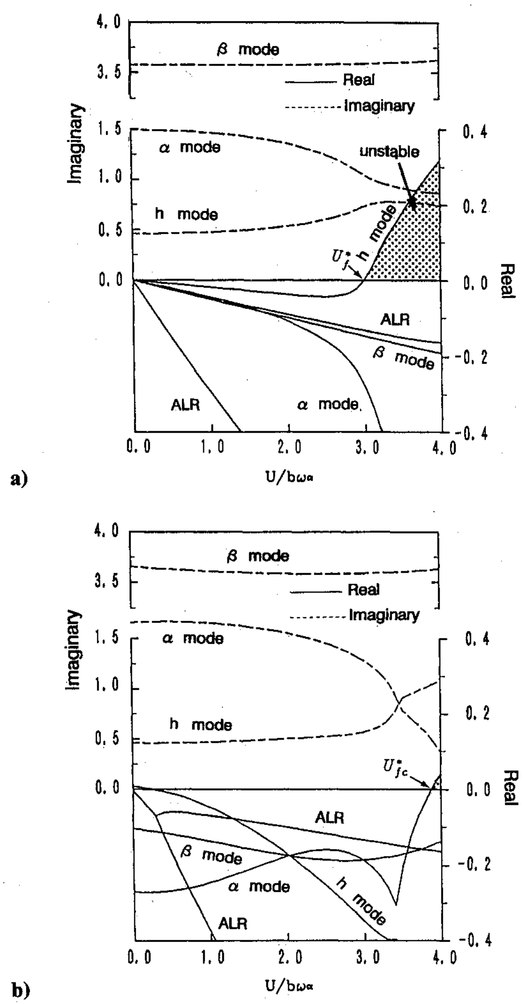

Fig. 8 Locus of nondimensional eigenvalues of final design: a) open-loop system; b) closed-loop system.

The y axis is the value of

$$\sum(w_j^+ d_j^+ + w_j^- d_j^-)$$

which indicates the achievement level of the goals in a given priority level. The first priority (stability requirements for both open- and closed-loop systems) and the second priority (restriction of the control surface deflection angle) are achieved early. The third priority (requirement for minimizing modifications) is satisfied as best as possible without decreasing the other two priorities. Figure 7 illustrates the histories of each design parameter. In the initial iterations, each parameter drastically changes to satisfy the first two priorities, then they later go to the initial values to minimize the design changes.

Table 3 Design parameters after modification

Design parameter	Initial value	Final value
χ_α	0.2	0.364
χ_β	0.0125	0.01248
a	−0.4	−0.449
c	0.5	0.461
U_D^*	3.25	3.514

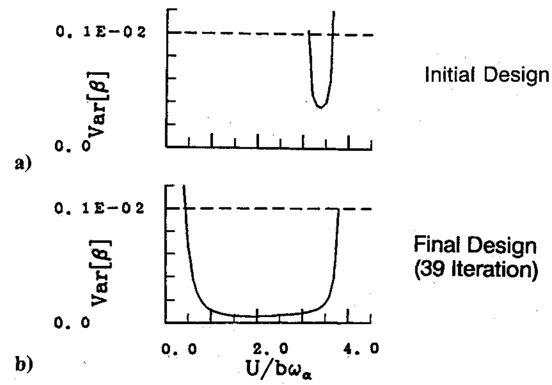

Fig. 9 Steady-state covariance of control surface deflection angle: a) initial design; b) final design (39 iterations).

The optimized design parameters are listed in Table 3. The center of gravity moved aft to extend the stable boundary of closed-loop system, the elastic axis moved forward to improve the open-loop flutter speed, which was worsened by the movement of the center of gravity, and the size and the center of gravity of the control surface slightly changed to satisfy the deflection angle restrictions. Additionally, the design speed increased to maintain the flutter speed of the closed-loop system. Figure 8 shows the resulting eigenvalues for the open- and closed-loop systems. In the final design, the values of the flutter speed for the open- and closed-loop systems were 3.00 and 3.88, respectively. Sufficient stability requirement characteristics for both systems were achieved. Figure 9 shows that the final design restrains the steady-state covariance of the control surface deflection angle.

Conclusions

The control and structure design parameters of a typical wing section with a trailing control surface were optimally modified to improve the dynamic characteristics in accordance with the following design requirements: the closed-loop system is stable over a wide range of flight speed without worsening the open-loop flutter speed, the control surface deflection angle is restrained, and the degree of structural design change is minimized. Sensitivity analysis was used to decompose the nonlinear optimization problem to a sequentially approximated linearized optimization problem. The simplex algorithm was applied to linearized goal programming problems to obtain the optimal modifications satisfying the multiple design requirements. Finally, note that future studies are needed to address more general design procedures. First, the presented study only considered a simple wing section model and neglected actuator dynamics and flow compressibility. Although, in a real situation, more detailed mathematical models are required, the method of sequential goal programming using the simplex algorithm is capable of handling a large number of design parameters and goals. Second, since a full-state feedback system used in the present paper is not feasible in general, a more general control system such as an acceleration based feedback system should be incorporated once the design procedure is completed.

References

[1]Newsom, J. R., "Control Law Synthesis for Active Flutter Suppression Using Optimal Control Theory," *Journal of Guidance and Control,* Vol. 2, No. 5, 1979, pp. 388–394.

[2]Mukhopadhyay, V., Newsom, J. R., and Abel, I., "Reduced Order Optimal Feedback Control Law Synthesis for Active Flutter Suppression," *Journal of Guidance and Control,* Vol. 4, No. 4, 1981, pp. 382–395.

[3]Liebst, B. S., Garrard, W. L., and Adams, W. M., "Design of an Active Flutter Suppression System," *Journal of Guidance, Control, and Dynamics,* Vol. 9, No. 1, 1986, pp. 64–71.

[4]Liebst, B. S., Garrard, W. L., and Farm, J. A., "Design of Multivariable Flutter Suppression/Gust Load Alleviation System," *Journal of Guidance, Control, and Dynamics,* Vol. 11, No. 3, 1988, pp. 220–229.

[5]Zeiler, T. A., and Weisshaar, T. A., "Integrated Aeroservoelastic Tailoring of Lifting Surface," *Journal of Aircraft,* Vol. 25, No. 1, 1988, pp. 76–83.

[6]Ashley, H., "Flutter Suppression within Reach," *Aerospace America,* Vol. 26, No. 8, 1988, pp. 14–20.

[7]Freymann, R., "Interaction Between an Aircraft Structure and Active Control System," *Journal of Guidance, Control, and Dynamics,* Vol. 10, No. 5, 1987, pp. 447–452.

[8]Lust, R. V., and Schmit, L. A., "Control-Augmented Structural Synthesis," *AIAA Journal,* Vol. 26, No. 1, 1988, pp. 86–95.

[9]Schaechter, D. B., "Closed-Loop Control Performance Sensitivity to Parameter Variations," *Journal of Guidance, Control, and Dynamics,* Vol. 6, No. 5, 1983, pp. 399–402.

[10]Lim, K. B., and Junkins, J. L., "Robustness Optimization of Structural and Controller Parameters," *Journal of Guidance, Control, and Dynamics,* Vol. 12, No. 1, 1989, pp. 89–96.

[11]Charnes, A., and Cooper, W. W., *Management Models and Industrial Applications of Linear Programming,* Vol. 1, Wiley, New York, 1961.

[12]Ignizo, J. P., *Goal Programming and Extensions,* Heath, Boston, MA, 1976.

[13]Steuer, R. E., *Multiple Criteria Optimization: Theory, Computation, and Application,* Wiley, New York, 1986.

[14]Edwards, J. W., Breakwell, J. V., and Bryson, A. E., Jr., "Active Flutter Control Using Generalized Unsteady Aerodynamic Theory," *Journal of Guidance and Control,* Vol. 1, No. 1, 1978, pp. 32–40.

[15]Edwards, J. W., Ashley, H., and Breakwell, J. V., "Unsteady Aerodynamic Modeling for Arbitrary Motions," *AIAA Journal,* Vol. 17, No. 4, 1979, pp. 365–374.

[16]Ohta, H., Fujimori, A., Nikiforuk, P. N., and Gupta, M. M., "Active Flutter Suppression for Two-Dimensional Airfoils," *Journal of Guidance, Control, and Dynamics,* Vol. 12, No. 2, 1989, pp. 188–194.

[17]Kwakernaak, H., and Sivan, R., *Linear Optimal Control Systems,* Wiley-Interscience, New York, 1972.

[18]Suzuki, S., and Matsuda, S., "Sensitivity Analysis of Typical Wing Section with Active Controller," *Proceedings of the 26th Aircraft Symposium of Japan Society for Aeronautical and Space Sciences,* JSAS, Tokyo, 1988, pp. 568–571 (in Japanese).

[19]Nelson, R. B., "Simplified Calculation of Eigenvector Derivatives," *AIAA Journal,* Vol. 14, No. 9, 1976, pp. 1201–1205.